

## Spatially modulated phases in AANNDI (axial antisymmetrical nearest-neighbour double Ising) models

This article has been downloaded from IOPscience. Please scroll down to see the full text article.

1992 J. Phys.: Condens. Matter 4 2609

(<http://iopscience.iop.org/0953-8984/4/10/022>)

View [the table of contents for this issue](#), or go to the [journal homepage](#) for more

Download details:

IP Address: 171.66.16.159

The article was downloaded on 12/05/2010 at 11:29

Please note that [terms and conditions apply](#).

## Spatially modulated phases in AANNDI (axial antisymmetrical nearest-neighbour double Ising) models

M Kurzyński† and M Bartkowiak‡§

† Institute of Physics, A Mickiewicz University, PL-60769 Poznań, Poland

‡ Division of Physics, The University of Trondheim (NTH), N-7034 Trondheim, Norway

Received 30 April 1991, in final form 30 October 1991

**Abstract.** The antisymmetrical interaction between nearest-neighbours in a statistical lattice model with two Ising variables can stabilize the long-period modulations of the order parameter. The range of stability of phases with the modulation period up to 13 lattice constants was found numerically in the molecular-field approximation. The model is supposed to explain the mechanism of transitions to long-period as well as incommensurate structures in  $A'A''BX_4$ -type compounds.

### 1. Introduction

The double Ising model with two variables  $\sigma = \pm 1$  and  $\tau = \pm 1$  was proposed some years ago [1, 2] for the interpretation of structural phase transitions in a number of compounds of a general chemical formula  $A'A''BX_4$ . Ferroelectric and ferroelastic transitions in these compounds, also involving long-period modulations, are supposed to result from various orientational orderings of  $BX_4$  groups. There are four possible orientations of each  $BX_4$  tetrahedron in the environment of A atoms, labelled jointly by the Ising variables  $\sigma$  (positions of the tetrahedron with one of apices up or down the hexagonal axis) and  $\tau$  (turns to the right or left about this axis). Symmetry implies the most general form of nearest neighbour (NN) interactions on the hexagonal close-packed (HCP) lattice to be

$$\begin{aligned}
 H = & J \sum_{\text{NN in}} \sigma_i \sigma_j + K \sum_{\text{NN in}} \tau_i \tau_j + L \sum_{\text{NN in}} \sigma_i \tau_i \sigma_j \tau_j + \frac{M}{2} \sum_{\text{NN in}} \sigma_i \sigma_j (\tau_i - \tau_j) \\
 & + J' \sum_{\text{NN out}} \sigma_i \sigma_j + K' \sum_{\text{NN out}} \tau_i \tau_j + L' \sum_{\text{NN out}} \sigma_i \tau_i \sigma_j \tau_j \\
 & + \frac{M'}{2} \sum_{\text{NN out}} \tau_i \tau_j (\sigma_i - \sigma_j)
 \end{aligned} \tag{1}$$

where 'NN in' and 'NN out' denote two kinds of nearest neighbours lying in and out of the hexagonal plane, respectively.

Symmetrical NN interactions ( $J, K, L, J', K', L'$ ) stabilize orderings with modulation period two at the most, and the model with only these interactions was successfully applied to the interpretation of all experimentally observed crystallographic

§ On leave from Institute of Physics, A Mickiewicz University, PL-60769 Poznań, Poland.

structures with up to four formula units per elementary cell [1, 2]. In a recent paper [3] it has been shown that the out-of-plane antisymmetrical interaction  $M'$  can stabilize ordering modulations of any period length along the hexagonal axis. Accordingly, the model is also able to explain the various long period as well as incommensurate structures observed in the considered class of compounds [4, 5]. Because interactions between NN are usually much stronger than those between next-nearest ones, it is natural to suppose that our model is more physically justified than a modified ANNNI (axial next-nearest-neighbour Ising) model [6] and a version of ELRII (effectively long-range interacting Ising) model [7] hitherto used for an explanation of modulated phases in  $A'A''BX_4$ -type compounds. The in-plane antisymmetrical interaction  $M$  is expected to explain the double- $k$  modulation in the hexagonal plane observed at high temperatures in  $\text{LiKSO}_4$  [4].

To follow the tradition of several-letter abbreviations we propose to call a statistical model involving the out-of-plane  $M'$  term, the AANNDI (axial antisymmetrical nearest-neighbour double Ising) model, and that involving the in-plane  $M$  term, the PANNDI (planar antisymmetrical nearest-neighbour double Ising) model. In a previous paper [3] only the existence of long-period modulated phases in the AANNDI model was shown. Here we present more details of the phase diagram found numerically in the molecular-field approximation (MFA).

## 2. Physical origin of antisymmetrical interactions

Formally, the existence of antisymmetrical interactions results from the lack of the centre of symmetry for NN pairs on the HCP lattice. The strengths of these interactions in the case of a rigid lattice is determined by purely electrostatic interactions between  $\text{BX}_4$  octopoles. In figure 1(a) two configurations of an NN pair of tetrahedra in the hexagonal plane are shown, one with  $\tau_1 = +1$ ,  $\tau_2 = -1$ , and the other with  $\tau_1 = -1$ ,  $\tau_2 = +1$ . It is obvious that, notwithstanding that  $\tau_1\tau_2 = -1$  in both cases, the electrostatic energy of the first configuration differs from that in the second. The simplest term describing the energy difference is  $(\tau_1 - \tau_2)$ , but it cancels with other such terms after summation along the whole chain of tetrahedra. The translational symmetry of the chain can be destroyed due to particular  $\sigma$ -orderings which yield various signs of the products  $\sigma_i\sigma_{i+1}$  for subsequent pairs. Consequently, it is only the antisymmetrical interaction of the form  $\sigma_1\sigma_2(\tau_1 - \tau_2)$  that discriminates between energies of both configurations and, simultaneously, may not cancel after summation.

Similarly, in figure 1(b) two configurations are shown of an NN pair of tetrahedra out of the hexagonal plane. Their electrostatic energy is different again and can be distinguished only by the antisymmetrical interaction of the form  $\tau_1\tau_2(\sigma_1 - \sigma_2)$ , possibly not cancelling after summation.

## 3. Simplifications and analytical results

Because of the complex topology of the HCP lattice and because our goal is to analyse the effects of the out-of-plane interaction  $M'$ , possibly, in relation to the Ising interactions  $J'$  and  $K'$ , we consider the mean-field free energy of Hamiltonian

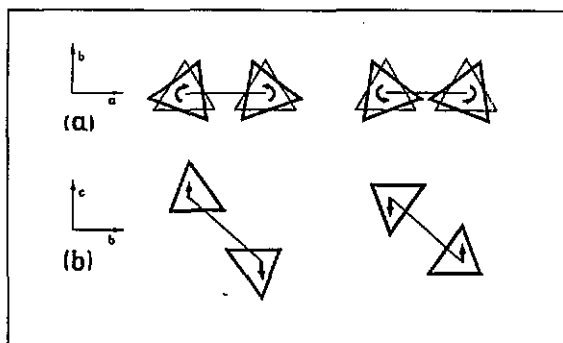


Figure 1. Two configurations of NN pairs of  $BX_4$  tetrahedra in the hexagonal plane (a) and out of the hexagonal plane (b), whose energies differ by the term of antisymmetrical interaction  $\frac{1}{2}M\sigma_1\sigma_2(\tau_1 - \tau_2)$  (a) and  $\frac{1}{2}M'\tau_1\tau_2(\sigma_1 - \sigma_2)$  (b). Notation of axes as in [1].

(1) in the form

$$\begin{aligned}
 FN^{-1} = & \tilde{J} \sum_l \sigma_l \sigma_{l+1} + \tilde{K} \sum_l \tau_l \tau_{l+1} + \frac{\tilde{M}}{2} \sum_l (\omega_l \tau_{l+1} - \tau_l \omega_{l+1}) \\
 & + \frac{1}{2} kT \sum_l [(1 + \sigma_l) \ln(1 + \sigma_l) + (1 - \sigma_l) \ln(1 - \sigma_l)] \\
 & + \frac{1}{2} kT \sum_l [(1 + \tau_l) \ln(1 + \tau_l) + (1 - \tau_l) \ln(1 - \tau_l)] \\
 & + \frac{1}{2} kT \sum_l [(1 + \omega_l) \ln(1 + \omega_l) + (1 - \omega_l) \ln(1 - \omega_l)]. \quad (2)
 \end{aligned}$$

Here the index  $l$  labels the successive parallel planes, and  $\sigma_l$ ,  $\tau_l$  and  $\omega_l$  are values of the (normalized to unity) layer order parameters:

$$\sigma_l \equiv N^{-1} \sum_p \langle \sigma_{lp} \rangle \quad \tau_l \equiv N^{-1} \sum_p \langle \tau_{lp} \rangle \quad \omega_l \equiv N^{-1} \sum_p \langle \sigma_{lp} \tau_{lp} \rangle \quad (3)$$

where the index  $p$  runs over all  $N$  sites in a given layer. The effective parameters  $\tilde{J}$ ,  $\tilde{K}$  and  $\tilde{M}$  depend not only on the number of NNS and parameters  $J'$ ,  $K'$  and  $M'$ , respectively, but also on the remaining parameters of Hamiltonian (1) and, moreover, on temperature. We are, however, not concerned with a particular form of such a dependence here.

The ground-state phase diagram for our model is given in figure 2(a). We consider it to be exact since our MFA result coincides with the exact solution (obtained with the aid of the transfer-matrix method) of a corresponding one-dimensional model [3].

Two limiting cases can be discussed analytically by solving linearized molecular-field equations.

(i) The case  $\tilde{M} \ll \tilde{J}$ . In the absence of coupling there is a continuous phase transition at the temperature

$$kT_\sigma = 2\tilde{J}$$

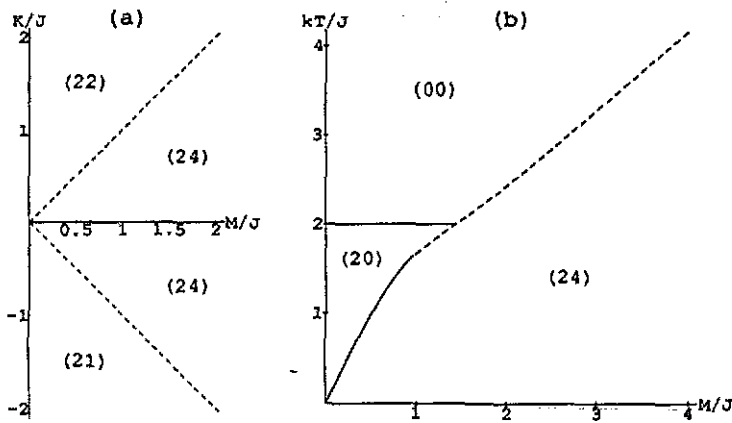


Figure 2. Ground-state phase diagram for  $\bar{J} > 0$  (a) and the cross section of a finite-temperature phase diagram for  $\tilde{K} = 0$  (b). The symbol  $(mn)$  is used to denote a phase with the modulation period  $m$  in the parameter  $\sigma$  and the modulation period  $n$  in the parameter  $\tau$  ( $m, n = 0$  means lack of appropriate ordering). The full and broken lines correspond to continuous and discontinuous phase transitions, respectively.

from the para to antiferro-ordered in the parameter  $\sigma$  phase. Well below  $T_\sigma$  one can assume  $\sigma_l = (-1)^l$  so the  $\tau$ -ordering is described by the effective free energy

$$F_{\text{eff}} N^{-1} = \sum_l \left[ \tilde{K} + (-1)^l \tilde{M} \right] \tau_l \tau_{l+1} + \frac{1}{2} kT \sum_l \left[ (1 + \tau_l) \ln(1 + \tau_l) + (1 - \tau_l) \ln(1 - \tau_l) \right]. \tag{5}$$

It can be seen directly that for  $\tilde{M} > |\tilde{K}|$  this interaction stabilizes a phase with the modulation period 4 with a pattern of  $\tau$ -ordering  $(\dots + + - - + + - - \dots)$ . In general, the temperature of a continuous transition to any phase ordered in  $\tau$  is given by

$$kT_\tau = 2\sqrt{\tilde{K}^2 \cos^2 q + \tilde{M}^2 \sin^2 q} \tag{6}$$

with  $q$  chosen to maximize this expression, i.e.  $q = 0$  for  $\tilde{K} < -\tilde{M}$ ,  $q = \pi/2$  for  $-\tilde{M} < \tilde{K} < \tilde{M}$ , and  $q = \pi$  for  $\tilde{K} > \tilde{M}$ .

(ii) The case  $\tilde{M} \gg \bar{J}$  was discussed in [3]. At the temperature

$$kT_{\sigma\tau} = -\tilde{K} \cos q + \sqrt{\tilde{K}^2 \cos^2 q + \tilde{M}^2 \sin^2 q} \tag{7}$$

there is a continuous phase transition from the para phase to the phase simultaneously ordered in  $\sigma$  and  $\tau$ . To maximize expression (7), the modulation vector has to be  $q = 0$  for  $\tilde{K} < -\tilde{M}/\sqrt{2}$  and  $q = \pi$  for  $\tilde{K} > \tilde{M}/\sqrt{2}$ . Within the range  $-\tilde{M}/\sqrt{2} < \tilde{K} < \tilde{M}/\sqrt{2}$  the maximizing value of  $q$  varies continuously from 0 to  $\pi$ , which means that points  $\tilde{K} = \pm\tilde{M}/\sqrt{2}$ , corresponding to temperature  $kT = \sqrt{2} \tilde{M}$ , are Lifshitz points.

#### 4. Numerical phase diagram

The analysis of the limiting cases has been carried out under the assumption that all phase transitions are continuous. This assumption can, however, no longer be valid in an intermediate region. Indeed, the numerically found finite-temperature phase diagram in  $\tilde{K} = 0$  plane, given in figure 2(b), shows that, for finite values of  $\tilde{M}/\tilde{J}$ , the transition to phase (24) becomes discontinuous. In figure 3 three representative cross sections of finite-temperature phase diagrams with  $\tilde{M}/\tilde{J} = \text{constant}$  are given. Only half-planes are shown, as the free energy (2) has a gauge symmetry

$$\tilde{K}, \tau_l \rightarrow -\tilde{K}, (-1)^l \tau_l. \quad (8)$$

It is seen that for  $\tilde{M}/\tilde{J} = 0.5$ , when transitions are still continuous, the numerical phase diagram agrees almost exactly with the analysis done in (i). The opposite limit, (ii), is, however, not reached even for  $\tilde{M}/\tilde{J} = 4.0$ . The discontinuity of the transition between the para phase (00) and the phase with  $q = 2\pi/4$  (24) results in a considerable reduction of the region of stability of phases with  $q \neq 2\pi/4$ , denoted in figure 3(c) as MP. In accordance with figure 3(c) we would like to note an mistake in the determination of the line separating phase (01) from MP in [3].

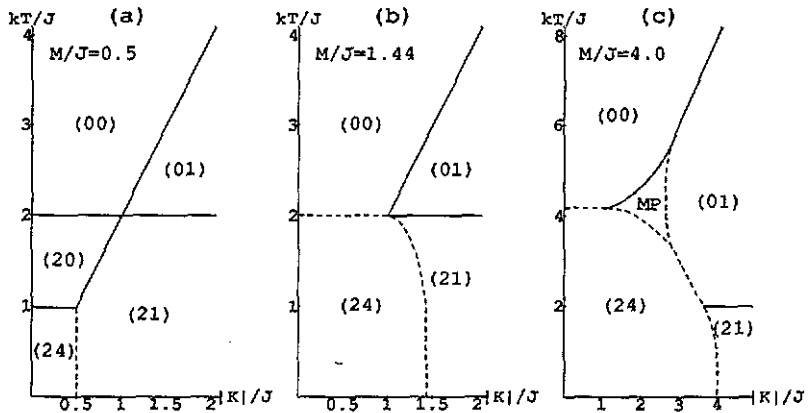


Figure 3. Three cross sections of the finite-temperature phase diagram with  $\tilde{M}/\tilde{J} = 0.5$  (a),  $\tilde{M}/\tilde{J} = 1.44$  (b), and  $\tilde{M}/\tilde{J} = 4.0$  (c). Notation as in figure 2. Phases (01) and (21) occur for  $\tilde{K} < 0$ ; for  $\tilde{K} > 0$ , they are replaced by phases (02) and (22), respectively. The area denoted by MP is a region of stability of long-period modulated phases.

Stability regions of phases with particular modulation vectors are shown in figure 4. The phase diagram has been constructed by comparing the free energies calculated for the solutions of thirteen systems of coupled nonlinear molecular-field equations, each for  $3n$  ( $n = 1, 2, \dots, 13$ ) variables  $\sigma_l, \tau_l$  and  $\omega_l$  ( $l = 1, 2, \dots, n$ ) satisfying periodic conditions  $\dots_{l+n} = \dots_l$ . For each  $n$ , the molecular-field equations have been solved numerically by means of an iteration procedure. As the starting spin configuration a sinusoidal structure, the self-consistent solution at a nearby temperature or (for low enough temperatures) the exact solution at the ground state have been used. Usually, the self-consistency has been obtained after some hundred iterations, but for certain values of  $n$  and  $T$  the convergence was very slow and near 50 000 iterations were needed. For some values of  $\tilde{K}$  and  $T$  the thirteen systems of equations have had

up to about 200 different solutions. It should be pointed out that the long-period solutions do not occur in the previously applied [1] approximation of the statistical independence of the  $\sigma$  and  $\tau$  subsystems

$$\langle \sigma_i \tau_i \rangle = \langle \sigma_i \rangle \langle \tau_i \rangle. \quad (9)$$

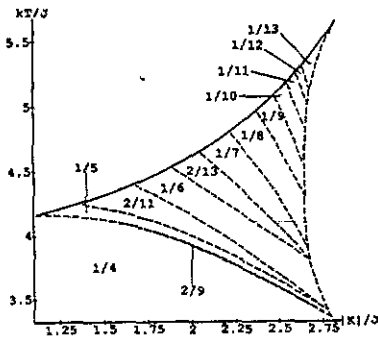


Figure 4. Enlargement of part of the diagram in figure 3(c). Stability regions of the phases with particular modulation vectors (given in units of the reciprocal lattice vector  $2\pi$ ) are indicated. The presented values of the modulation vector correspond to the case  $\tilde{K} < 0$ ; for  $\tilde{K} > 0$ , they should be replaced by the appropriate complements to  $\frac{1}{2}$ . All transitions, except that to the para phase, are discontinuous.

To complete the phase diagram of modulated phases an additional analysis of molecular-field equations in the soliton approximation is needed, as well as a low-temperature analysis of phase branching [8]. Studies of this kind using AANNDI model are in progress. We also expect to get interesting results in the molecular-field theory of the PANNDI model.

### Acknowledgments

This study has been supported by the Alexander von Humboldt Foundation (MK), by the Royal Norwegian Council for Scientific and Industrial Research (NTNF) (MB) and by the Institute for Low Temperatures and Structural Research of the Polish Academy of Sciences within project CPBP 01.12.

### References

- [1] Kurzyński M and Halawa M 1986 *Phys. Rev. B* **34** 4846
- [2] Kurzyński M 1988 *Ferroelectrics* **78** 121
- [3] Kurzyński M, Ossowski M and Bartkowiak M 1990 *Ferroelectrics* **105** 107
- [4] Cummins H Z 1990 *Phys. Rep.* **185** 211
- [5] Kurzyński M 1992 *Ferroelectrics* at press
- [6] Yamada Y and Hamaya N 1983 *J. Phys. Soc. Japan* **52** 3466
- [7] Kawamura K, Kuramashi A, Nakamura H, Kasano H, Mashiyama H, Nakanishi S and Itoh H 1990 *Ferroelectrics* **105** 279